Journal Article

CdTe thin film solar cells produced using a chamberless inline process via metalorganic chemical vapour deposition

Kartopu, G., Barrioz, V., Monir, S., Lamb, D.A. and Irvine, S.J.C.

CdTe thin film solar cells produced using a chamberless inline process via metalorganic chemical vapour deposition

G. Kartopu*, V. Barrioz, S. Monir, D.A. Lamb and S.J.C. Irvine
Centre for Solar Energy Research (CSER), Glyndŵr University, St. Asaph, LL17 0JD, UK

$Cd_{1-x}Zn_xS$ and CdTe:As thin films were deposited using a recently developed chamberless inline process using metalorganic chemical vapour deposition (MOCVD) at atmospheric pressure and assessed for fabrication of CdTe photovoltaic (PV) solar cells. Initially, CdS and $Cd_{1-x}Zn_xS$ coatings were applied onto 15 × 15 cm^2 float glass substrates, characterised for their optical properties, and then used as the window layer in CdTe solar cells which were completed in a conventional MOCVD (batch) reactor. Such devices provided best conversion efficiency of 13.6% for $Cd_{0.36}Zn_{0.64}S$ and 10% for CdS which compare favourably to the existing baseline MOCVD devices. Next, sequential deposition of $Cd_{0.36}Zn_{0.64}S$ and CdTe:As films were realised by the chamberless inline process. The chemical composition of a 1 µm CdTe:As/150 nm $Cd_{0.36}Zn_{0.64}S$ bi-layer was observed via secondary ions mass spectroscopy, which showed that the key elements are uniformly distributed and the As doping level is suitable for CdTe device applications. CdTe solar cells formed using this structure provided a best efficiency of 11.8% which is promising for a reduced absorber thickness of 1 µm. The chamberless inline process is non-vacuum, flexible to implement and inherits from the legacy of MOCVD towards doping/alloying and low temperature operation. Thus, MOCVD enabled by the chamberless inline process is shown to be an attractive route for thin film PV applications. **Keywords:** *Chamberless inline process; (AP)MOCVD; CdTe thin film PV.*

* Corresponding author, Dr. Giray Kartopu. E-mail: giray.kartopu@glyndwr.ac.uk.
Tel: +44-1745-535-213. Address: CSER, Ffordd William Morgan, OpTIC Glyndŵr,
St. Asaph Business Park, North Wales, LL17 0JD, UK.

1. INTRODUCTION

Among several thin film deposition techniques, metalorganic chemical vapour deposition (MOCVD) is an attractive route for thin film photovoltaic (PV) applications as it offers flexibility for material engineering via doping/alloying and the capability to produce functional coatings at atmospheric pressure. MOCVD is commonly associated with epitaxial III-V multi-junction solar cells [1,2], but it is also shown to be capable of producing low cost superstrate devices of polycrystalline CdTe with promising device performance [3].

Thin film CdTe PV maintains its dominant position within thin film PV technologies, with a total share of the global PV market of ~6% in 2013 [4]. Industrial CdTe PV modules are currently fabricated primarily using vapour transport deposition process but requires a vacuum and relatively high temperature (>500 °C) operation. Nevertheless, this process has been demonstrated by First Solar to yield high efficiency devices (20.4% for cells and 17% for modules [5]) with relatively low production cost ($\$0.68/W_p$).

The suitability of MOCVD for the inline deposition of semiconductor thin films was recently assessed using a coating head arrangement with the normal-to-substrate injector geometry [6,7]. An improved material utilisation efficiency of 40% was demonstrated for deposition of CdTe thin films in comparison to conventional (horizontal) MOCVD process. This process was still carried out in a sealed reaction chamber over relatively small (5×7.5 cm^2) substrates and yielded a best device efficiency of ~11%. In this study, a chamberless inline process (CIP) based on atmospheric pressure MOCVD, developed by the Centre for Solar Energy Research [8], was used to apply $Cd_{1-x}Zn_xS$ and CdTe coatings over 15×15 cm^2 glass substrates and assessed, for the first time, in CdTe PV solar cells.

2. EXPERIMENTAL DETAILS

The inline system was designed to operate a number of coating heads for sequential deposition of all the active components in a typical CdTe PV device structure. In the case of baseline MOCVD devices (Fig. 1), these include a transparent conducting oxide (TCO) layer as the front contact, $Cd_{1-x}Zn_xS$ layer as the window, p-CdTe absorber, p^+-CdTe as the back contact layer (BCL) followed by the $CdCl_2$ deposition and activation anneal. $CdCl_2$ acts as the catalyst and excess is removed after the anneal treatment.

Figure 2 illustrates the operation principle of the CIP. The substrate (15 × 15 cm^2), housed within a graphite susceptor, is translated using a linear stage at constant speeds (adjustable) underneath the coating heads where the chemical reaction takes place. The process gas (H_2 used in this study) with the metalorganic precursors are introduced through an injector slit (inlet) and impinge upon the moving and heated substrate, where the solid product of reaction forms. The chemical by-products are extracted from the reaction zone encompassed by an exhaust (outlet). The reaction zone is contained by means of a nitrogen curtain. The nitrogen curtain maintains the integrity of the reaction zone by preventing ingress of ambient atmosphere and escape of gases from the reaction zone. Further details of the coating head design and its performance are provided elsewhere [8, 9].

A commercial TCO coated glass (NSG TEC^{TM} C10) was used as the substrate in this study. Dimethylcadmium (DMCd), ditertiarybutyl-sulfide (DtBS) and diethylzinc (DEZn) precursors obtained from SAFC Hitech were used to deposit the window layers (i.e. CdS or $Cd_{1-x}Zn_xS$) at a substrate temperature (T_s) of 380 °C. A single pass, at 1.8 cm·min^{-1} translation speed, produced 130 ± 30 nm coatings on the substrate for precursor concentrations 2.6 × 10^{-3} atm (DMCd), 1.2 × 10^{-3} atm (DtBS) and 1.4 × 10^{-3} atm (DEZn)

within a total flow of 1 l·min^{-1}. The chemical purity and optical properties of the coatings were characterised using energy dispersive X-ray analysis (Hitachi TM3000 SEM, 15kV electron energy) and optical transmittance (Varian Cary 5000 spectrometer, 200-900 nm scan range) measurements, respectively. The bandgap of $Cd_{1-x}Zn_xS$ thin films was calculated by plotting the absorption constant (α) vs. energy (E) relationship, i.e. α^2E^2 vs. E, which was then compared to the literature [10,11] to determine the film composition. Arsenic doped CdTe films were also deposited in a single pass and at the same speed, with T_s = 430 °C. The precursors for Te and As were diisopropyltelluride (DiPTe) and tris(dimethylamino)arsenic (tDMAAs), respectively. For precursor concentrations of 4.6 × 10^{-3} atm (DMCd), 1.4 × 10^{-3} atm (DiPTe), and 7.5 × 10^{-6} atm (tDMAAs) and total flow of 1 l·min^{-1} typical film thickness was 1 μm for this CdTe layer.

A portion of the 15 × 15 cm^2 samples was processed as devices, with the device structure/activation completed in the batch MOCVD reactor. Formation of hybrid devices was useful to establish the compatibility of the chamberless technique in comparison with the well-established material deposited by the batch reactor [7]. Further coating heads for TCO, p^+-CdTe BCL and $CdCl_2$ deposition will be implemented at a later stage in this research. The first set of hybrid devices evaluated the window layer deposited by the CIP. This required the deposition of a p-CdTe absorber (2000 nm), p^+-CdTe BCL (250 nm), and carrying out the $CdCl_2$ activation in the batch reactor. The final device structure was *npp*$^+$ type as shown in Fig. 1. A second set assessed sequentially deposited CdTe:As/$Cd_{1-x}Zn_xS$ *p-n* junctions, whereby only the p^+-CdTe BCL deposition and $CdCl_2$ activation were carried out on the batch reactor. For optimum device performance, targeted As doping levels are ~10^{18} and >10^{19} atoms·cm^{-3} for the bulk CdTe absorber and the p^+-CdTe BCL, respectively [3]. The precursors remained the same while their partial pressures were 0.2 × 10^{-3} atm (DMCd),

0.1×10^{-4} atm (DiPTe), and 1.0×10^{-6} atm (tDMAAs) for a total flow of 4.4 l·min^{-1}, with T_s = 395 °C for CdTe:As deposition when moving to the batch reactor. Device activation was achieved by depositing a $CdCl_2$ layer at 200 °C, using tertiarybutylchloride as the Cl source, and annealing at 420 °C under the prevalent H_2 atmosphere. A secondary post-deposition activation anneal was also performed for 30 min in ambient air (i.e. oxygen containing environment) at 170 °C [12]. The back contacts were then defined via thermal evaporation of Au through a shadow mask, defining individual solar cells of 0.25 cm^2.

Current density-voltage (J-V) measurements were carried out under AM1.5 illumination using an ABET 2000 solar simulator calibrated using a crystalline silicon cell certified by Fraunhofer Institute. Spectral response (external quantum efficiency, EQE) was measured using a Bentham PV300 spectrometer following the calibration of the system response using a certified silicon photodetector. For secondary ion-mass spectroscopy (SIMS) depth profiles of As^{75} (and other reference isotopes), a Cameca IMS-4f instrument with Cs^+ ion source operating with 10 keV energy and 20 nA current was used. A 1 × 1 cm^2 specimen was cleaved and etched in a diluted bromine/methanol solution to reduce surface roughness prior to SIMS measurements.

Device parameters were also modelled as a function of absorber thickness using SCAPS, a one-dimensional solar cell simulation programme [13]. In these simulations, the $Cd_{1-x}Zn_xS$ window layer absorption characteristics were introduced from the experimental spectral response (EQE) of a baseline CdTe device produced by horizontal MOCVD reactor, employing a 150 nm $Cd_{0.4}Zn_{0.6}S$ nominal window layer. For each device simulation, the shunt resistance (R_{sh}) calculated from the light J-V curve as well as the window layer thickness was input to improve the accuracy of the modelling. The experimental sample

thickness for each device was measured by dektak profilometry after chemically etching away the material surrounding each device which was protected by an electrical tape. Deducting the thickness due the window layer (100-150 nm) and p^+-CdTe BCL (250 nm) gave an estimate of the bulk p-CdTe thickness (an error of ±100 nm is assumed in each case). The thickness distribution of an inline MOCVD coating is controlled by the uniformity of precursor delivery and heating of the substrate. These in turn are dependent on the type and geometry of substrate holder, the coating head alignment and its openings (due to injector nozzle and extraction/curtain flows).

3. RESULTS AND DISCUSSION

3.1 Solar cells formed using inline $Cd_{1-x}Zn_xS$ window layers

The composition vs. bandgap relationship of the $Cd_{1-x}Zn_xS$ alloy system usually given by

$$E_g(x) = E_g(\mathrm{CdS}) + [E_g(\mathrm{ZnS}) - E_g(\mathrm{CdS}) - b]x + bx^2 \quad (1)$$

where $E_g(\mathrm{CdS}) = 2.42$ eV, $E_g(\mathrm{ZnS}) = 3.54$ eV, and b the bowing parameter (0.91 eV) [10]. A previous study showed that MOCVD $Cd_{1-x}Zn_xS$ films obey this description [11]. Transmittance behaviour of two inline window layers selected for device applications is presented in Fig. 3. The optical gap of the $Cd_{1-x}Zn_xS$ sample (160 nm), which shows a sharp short-wavelength cut-off, can be determined to be 2.9 eV. Following Eqn. 1, this corresponds to $x = 0.64$, i.e. $Cd_{0.36}Zn_{0.64}S$. The uniform band-edge observed for this sample is encouraging as it indicates single, uniform composition that is achieved by the CIP without requirement of a CdS/$Cd_{1-x}Zn_xS$ bi-layer structure needed in the batch reactor [10,14]. The CdS sample (100 nm) shows a short wavelength cut-off near ~500 nm (2.4 eV bandgap) with a tail in the blue/ultraviolet region, resulting from the reduced thickness. 100 nm and thinner CdS films

are commonly employed in thin film CdTe solar cells [15,16], which help to maintain the photocurrent by partially transmitting the high energy photons to the absorber.

Table 1 compares the J-V characteristics of ~100 nm CdS and $Cd_{0.36}Zn_{0.64}S$ based solar cells. While the CdS devices yielded mean and best efficiency of 8.6 ± 0.9% and 10.0%, respectively, the $Cd_{1-x}Zn_xS$ devices provided 12.7 ± 0.9% mean and 13.6% best efficiency. (As a control, a CdTe device without any window layer produced a short circuit current density, J_{sc} of 12 mA/cm^2, open circuit voltage, V_{oc} of 230 mV, and fill factor, FF of 31%.) The better performance of the $Cd_{0.36}Zn_{0.64}S$ solar cells is chiefly due to the higher J_{sc} produced by these devices (by ~5 mA·cm^{-2}), as can be inferred from the representative light J-V curves and EQE spectra given in Fig. 4. The blue-response is clearly enhanced with the incorporation of Zn into the CdS structure. The EQE of the $Cd_{0.36}Zn_{0.64}S$ device also shows a double-edge appearance at short wavelengths which is due to the low window layer thickness (≤100 nm). The difference in $Cd_{0.36}Zn_{0.64}S$ thickness between Figs. 3 and 4 is most likely due to the spread in the deposited material thickness as mentioned above. The high shunt resistance (R_{sh}) recorded for all devices (≥1000 Ω cm^2) is indicative of good nucleation and coverage of the inline window layers.

3.2 Inline CdTe:As/$Cd_{1-x}Zn_xS$ p-n junction devices

A (1 μm) CdTe:As/(150 nm) $Cd_{0.36}Zn_{0.64}S$ *p-n* junction structure formed by sequential layer deposition by the CIP was tested in solar cells. SIMS depth profiling of certain key elements in this structure (Fig. 5) verified a uniform distribution of the chemical constituents. The CdTe appears to be thinner than the starting value (1 μm) due to the chemical etching applied prior to the measurements. The As concentration is of the order of 2×10^{18} atoms·cm^{-3} which is close to the bulk values reported for CdTe:As solar cells produced by the MOCVD batch

reactor [3]. The rise of the Te^{120} signal towards the TCO layer is an artefact of the Sn^{120} signal emanating from the fluorine-doped tin oxide TEC^{TM} C10 [7]. Further structural analysis data (SEM and X-ray diffraction) for the inline CdTe films were reported in Ref. 9. By analysing the available data, the apparent grain size (from SEM images) and mean crystallite size (from the 111-CdTe reflection in the X-ray diffraction pattern) were estimated to be ~330 nm and ~70 nm, respectively. A similar crystallite size (~50 nm) can be calculated for the batch MOCVD samples reported in Ref. 7. Both the grain size and crystallite size are expected to increase upon device activation following the $CdCl_2$ treatment [14].

Following the deposition of the 250 nm p^+-CdTe BCL and cell activation as described above, J-V and EQE response of the solar cells were obtained (Table 2 and Fig. 6). Due mainly to the reduced absorber thickness of ~1.25 μm, e.g. compared to devices presented in the previous section, the EQE level is reduced with a maximum of ~80% at shorter wavelengths and further losses at longer wavelengths. Nevertheless, the FF and V_{oc} compare favourably to those of the $Cd_{0.36}Zn_{0.64}S$ based devices in Table 1 which used an absorber of 2.25 μm. The quality of the absorber grown by the CIP appears to be comparable to that of the batch MOCVD reactor despite the much higher deposition rate. It is also clear from the EQE spectra that the $Cd_{0.36}Zn_{0.64}S$ window layer is relatively thicker (by ~50 nm) for the inline *p-n* junction device, which adds to photocurrent loss observed with this device.

Fig. 7 compares the J_{sc} of inline produced hybrid devices (with $Cd_{0.36}Zn_{0.64}S$ window) in relation to total absorber thickness measured for each device. For the simulated J_{sc} the current loss with reducing CdTe thickness is not as steep as that seen by the J_{sc} calculated from the J-V curve. Thus, the J_{sc} loss of 3-4 $mA \cdot cm^{-2}$ observed for the *p-n* junction device compared to other hybrid devices may be attributed to the following effects; (a) thinner absorber layer, (b)

thicker window layer, (c) increased carrier recombination at the interfaces and grain boundaries. The performance of fully inline *p-n* junction devices could therefore potentially be improved by adjusting the window and absorber thickness, e.g. through precursor concentration, substrate translation speed or multiple injector arrangement. Further work is ongoing to realise the growth of all active layers needed in a CdTe device (Fig. 1); results of this work and optimisation of layer properties will be the subject of future studies.

4. CONCLUSION

A chamberless inline process based on atmospheric pressure MOCVD was used to deposit $Cd_{1-x}Zn_xS$ and CdTe:As thin films for PV applications. Solar cells fabricated using inline deposited ~100 nm CdS and $Cd_{0.36}Zn_{0.64}S$ window layers resulted in 10 % and 13.6 % best efficiency, respectively. The major gain introduced by Zn alloying of the window layer was the enhanced device blue response which resulted in a ~5 $mA \cdot cm^2$ increase in photocurrent. The chemical structure of an inline grown (1 µm) CdTe:As/(150 nm) $Cd_{0.36}Zn_{0.64}S$ sample showed uniform chemical composition with desirable level of As concentration achieved in the CdTe layer. The device performance of this *p-n* junction was limited by the reduced absorber thickness (~1.25 µm including the BCL) and slightly thicker window layer, but a promising best efficiency of 11.8% was reached. Preparation and further development of PV devices grown entirely by the chamberless inline process are in progress.

Acknowledgements

The coating head and chamberless inline system was built during the Solar Photovoltaic Academic Research Consortium (SPARC) project, gratefully funded by the European Regional Development Fund (ERDF) through Low Carbon Research Institute (LCRI). ESF and Scanwel Ltd. are also thanked for funding a Knowledge Economy Skills Scholarship (KESS).

REFERENCES

[1] R. L. Moon, MOVPE: is there any other technology for optoelectronics?, J. Cryst. Growth 170 (1997) 1-10.

[2] S. Rushworth, High Purity Metalorganic Precursors for CPV Device Fabrication, Mater. Matters 5 (4) (2010) 94-98.

[3] S.J.C. Irvine, V. Barrioz, D. Lamb, E.W. Jones, R.L. Rowlands-Jones, MOCVD of thin film photovoltaic solar cells - Next generation production technology?, J. Cryst. Growth 310 (2008) 5198-5203.

[4] NPD Solarbuzz PV Equipment Quarterly, 2013, http://www.solarbuzz.com/reports/pv-equipment-quarterly.

[5] M.A. Green, K. Emery, Y. Hishikawa, W. Warta, E.D. Dunlop, Solar cell efficiency tables (version 44), Prog. Photovolt: Res. Appl. 22 (2014) 701.

[6] V. Barrioz, G. Kartopu, S.J.C. Irvine, S. Monir, X. Yang, Material utilisation when depositing CdTe layers by inline AP-MOCVD, J. Cryst. Growth 354 (2012) 81-85.

[7] G. Kartopu, V. Barrioz, S.J.C. Irvine, A.J. Clayton, S. Monir, D.A. Lamb, Inline atmospheric pressure metal-organic chemical vapour deposition for thin film CdTe solar cells, Thin Solid Films 558 (2014) 374-377.

[8] V. Barrioz, D.A. Lamb, S. Monir, S. Trueman, G. Kartopu, I.W. Owen, S.J.C. Irvine, X. Yang, UK Patent Application (GB1302306.4); PCT patent application (PCT/GB2014/050386).

[9] V. Barrioz, G. Kartopu, S. Monir, D.A. Lamb, W. Brooks, A.J. Clayton, P. Siderfin and S.J.C. Irvine, MOCVD for solar cells, a transition towards a chamberless inline process, J. Cryst. Growth (to be published).

[10] W. Xia, J.A. Welt, H. Lin, H.N. Wu, M.H. Ho, C.W. Tang, Fabrication of $Cd_{1-x}Zn_xS$ films with controllable zinc doping using a vapor zinc chloride treatment, Sol. Energ. Mat. Sol. C. 94 (2010) 2113-2118.

[11] G. Kartopu, A.J. Clayton, W.S.M. Brooks, S.D. Hodgson, V. Barrioz, A. Maertens, D.A. Lamb, S.J.C Irvine, Effect of window layer composition in $Cd_{1-x}Zn_xS$/CdTe solar cells, Prog. Photovolt: Res. Appl. 22 (2014) 18-23.

[12] S. L. Rugen-Hankey, A. J. Clayton, V. Barrioz, G. Kartopu, S. J. C. Irvine, J. D. McGettrick, D. Hammond, Improvement to thin film CdTe solar cells with controlled back surface oxidation, Sol. Energ. Mat. Sol. C. (to be published).

[13] M. Burgelman, P. Nollet, S. Degrave, Modelling polycrystalline semiconductor solar cells, Thin Solid Films 361-362 (2000) 527-532.

[14] G. Kartopu, A. A. Taylor, A. J. Clayton, V. Barrioz, D. A. Lamb, S. J. C. Irvine, $CdCl_2$ treatment related diffusion phenomena in $Cd_{1-x}Zn_xS$/CdTe solar cells, J. Appl. Phys. 115 (2014) 104505-1–104505-5.

[15] T.L. Chu, S.S. Chu, C. Ferekides, C.Q. Wu, J. Britt, C. Wang, 13.4% efficient thin-film CdS/CdTe solar cells, J. Appl. Phys. 70 (12) (1991) 7608-7612.

[16] D.E. Swanson, R.M. Geisthardt, J.T. McGoffin, J.D. Williams, J.R. Sites, Improved CdTe Solar-Cell Performance by Plasma Cleaning the TCO Layer, IEEE J. Photovol. 3 (2013) 838-842.

LIST OF TABLES.

Table 1 Summary of the J-V characteristics of the CdTe superstrate solar cells based on inline deposited CdS and $Cd_{0.36}Zn_{0.64}S$ window layers.

	CdS/CdTe			CdZnS/CdTe		
	Best =	Mean =	σ =	Best =	Mean =	σ =
η (%)	10.0	8.6	0.9	13.6	12.7	0.9
J_{sc} (mA cm^{-2})	21.8	22.2	0.5	27.4	26.2	1.6
V_{oc} (mV)	687	660	18	727	723	23
FF (%)	66.5	58.9	4.8	68.4	67.1	3.6
R_s (Ω cm^2)	3.1	3.2	0.3	3.0	3.1	0.3
R_{sh} (Ω cm^2)	2008	1118	547	2512	1788	510

Table 2 J-V characteristics of an inline (1 μm) CdTe:As/(150 nm) $Cd_{0.36}Zn_{0.64}S$ thin film *p-n* junction, completed to full device structure utilising the batch MOCVD reactor.

	Best =	Mean =	σ =
η (%)	11.8	11.1	0.6
J_{sc} (mA cm^{-2})	23.1	22.9	0.7
V_{oc} (mV)	727	696	15
FF (%)	70.5	69.3	1.5
R_s (Ω cm^2)	2.9	2.8	0.2
R_{sh} (Ω cm^2)	728	737	121

FIGURE CAPTIONS.

Fig. 1 Typical MOCVD CdTe device structure.

Fig. 2 Schematic representation of the chamberless inline process used in the fabrication of CdTe solar cells. The substrate is translated using a linear stage underneath the coating head which is formed of an injector (inlet), a set of exhausts (outlet) and a nitrogen curtain delivery [8].

Fig. 3 Transmittance behaviour of representative window layers obtained by CIP and selected for device applications.

Fig. 4 (a) Light J-V curve and **(b)** spectral response (EQE) of typical CdTe devices fabricated using ~100 nm CdS and $Cd_{1-x}Zn_xS$ inline window layers. J-V response of a control device with no window layer (i.e. TCO/CdTe junction) is also shown for comparison. Note the improvement in blue-response due to alloying of CdS with ZnS, i.e. $Cd_{1-x}Zn_xS$, leading to ~5 $mA{\cdot}cm^2$ gain in the photocurrent.

Fig. 5 SIMS profile of Te^{120}, S^{36}, and As^{75} isotopes within a CdTe:As/$Cd_{1-x}Zn_xS$ bi-layer grown by the CIP and used in the device application.

Fig. 6 Typical EQE spectrum of the solar cells fabricated by using the inline grown (~1 μm) CdTe:As/(150 nm) $Cd_{0.36}Zn_{0.64}S$ bi-layer structure, shown in Fig. 5, in reference to that of a hybrid device employing inline $Cd_{0.36}Zn_{0.64}S$ window layer (also given in Fig. 4b). The full device is completed in a batch MOCVD reactor following the growth of p^+-CdTe BCL and $CdCl_2$ activation. The relatively low absorber thickness (~1.25 μm including BCL) appears to be the main cause of the reduced EQE (and J_{sc}) levels compared to the other hybrid device which uses a total 2.25 μm absorber and 100 nm window layer.

Fig. 7 The J_{sc} calculated from the J-V curve (**1**) and SCAPS simulation (**2**) for inline produced hybrid devices utilising a $Cd_{0.36}Zn_{0.64}S$ window layer. Data points in the 1.2-1.5 μm range belong to the devices fabricated using the inline deposited (~1 μm) CdTe:As/(150 nm) $Cd_{0.36}Zn_{0.64}S$ bi-layer while others are due to the hybrid device employing (100 nm) $Cd_{0.36}Zn_{0.64}S$ inline window layer. Broken lines are guide to the eye.

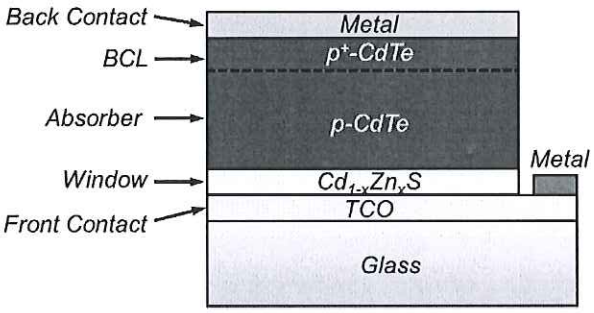

Fig. 1 Typical MOCVD CdTe device structure.

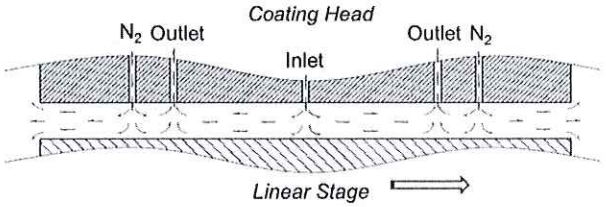

Fig. 2 Schematic representation of the chamberless inline process used in the fabrication of CdTe solar cells. The substrate is translated using a linear stage underneath the coating head which is formed of an injector (inlet), a set of exhausts (outlet) and a nitrogen curtain delivery [8].

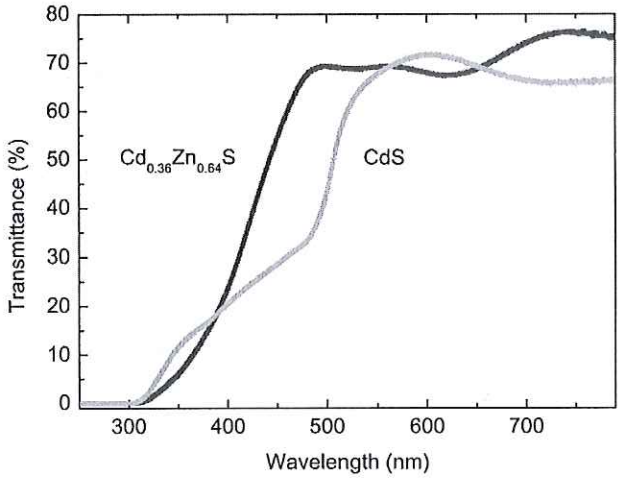

Fig. 3 Transmittance behaviour of representative window layers obtained by CIP and selected for device applications.

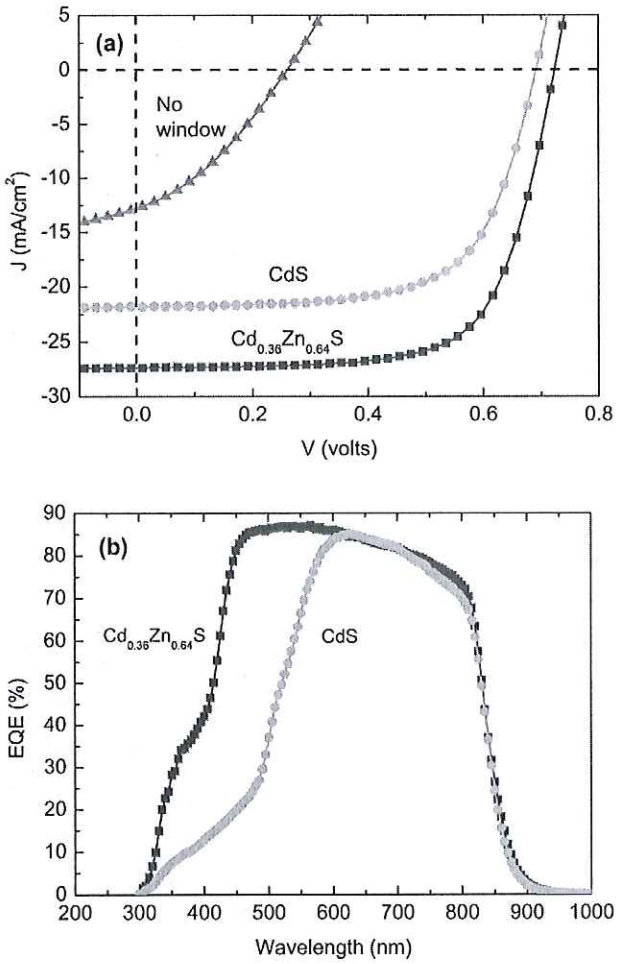

Fig. 4 (a) Light J-V curve and **(b)** spectral response (EQE) of typical CdTe devices fabricated using ~100 nm CdS and $Cd_{1-x}Zn_xS$ inline window layers. J-V response of a control device with no window layer (i.e. TCO/CdTe junction) is also shown for comparison. Note the improvement in blue-response due to alloying of CdS with ZnS, i.e. $Cd_{1-x}Zn_xS$, leading to ~5 mA·cm^2 gain in the photocurrent.

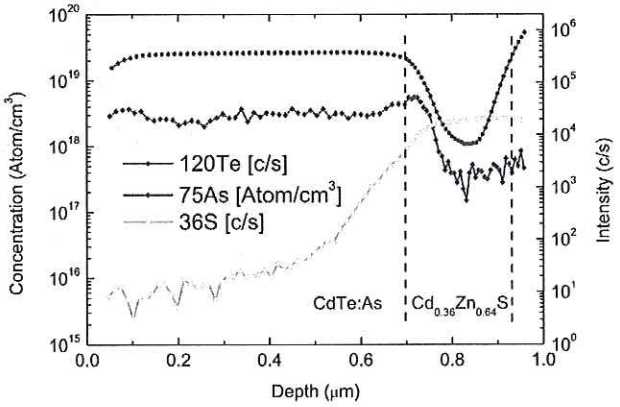

Fig. 5 SIMS profile of Te^{120}, S^{36}, and As^{75} isotopes within a CdTe:As/$Cd_{1-x}Zn_xS$ bi-layer grown by the CIP and used in the device application.

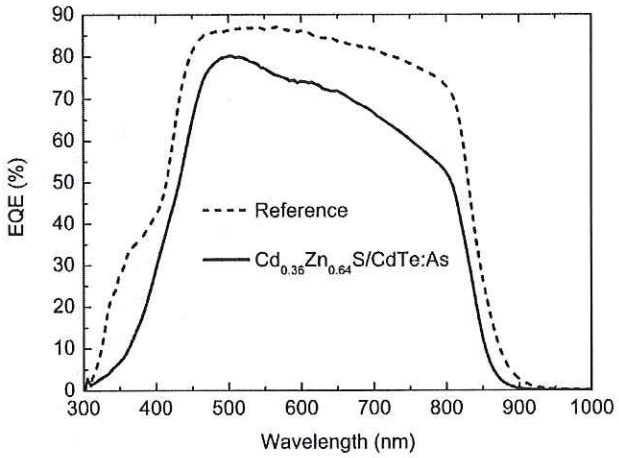

Fig. 6 Typical EQE spectrum of the solar cells fabricated by using the inline grown (~1 μm) CdTe:As/(150 nm) $Cd_{0.36}Zn_{0.64}S$ bi-layer structure, shown in Fig. 5, in reference to that of a hybrid device employing inline $Cd_{0.36}Zn_{0.64}S$ window layer (also given in Fig. 4b). The full device is completed in a batch MOCVD reactor following the growth of p^+-CdTe BCL and $CdCl_2$ activation. The relatively low absorber thickness (~1.25 μm including BCL) appears to be the main cause of the reduced EQE (and J_{sc}) levels compared to the other hybrid device which uses a total 2.25 μm absorber and 100 nm window layer.

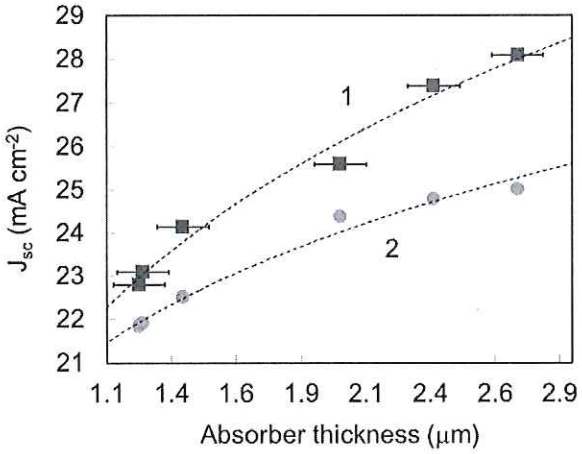

Fig. 7 The J_{sc} calculated from the J-V curve (**1**) and SCAPS simulation (**2**) for inline produced hybrid devices utilising a $Cd_{0.36}Zn_{0.64}S$ window layer. Data points in the 1.2-1.5 μm range belong to the devices fabricated using the inline deposited (~1 μm) CdTe:As/(150 nm) $Cd_{0.36}Zn_{0.64}S$ bi-layer while others are due to the hybrid device employing (100 nm) $Cd_{0.36}Zn_{0.64}S$ inline window layer. Broken lines are guide to the eye.